Electronic Supplementary Material (ESI) for New Journal of Chemistry

Surface quaternized nanosensor as an one-arrow-two-hawks approach for fluorescence turns "on-off-on" bifunctional sensing and antibacterial activity

Poushali Das[1], Sayan Ganguly[2], Madhuparna Bose[3], Debes Ray[4], Sabyasachi Ghosh[2], Subhadip Mondal[2], Vinod K Aswal[4], Amit Kumar Das[3], Susanta Banerjee[1,5], and Narayan Chandra Das[*,1,2].

[1]School of Nanoscience and Technology, Indian Institute of Technology, Kharagpur 721302
[2]Rubber Technology Centre, Indian Institute of Technology, Kharagpur 721302
[3]Department of Biotechnology, Indian Institute of Technology, Kharagpur 721302
[4]Solid State Physics Division, Bhabha Atomic Research Centre, Mumbai 400085, India
[5]Materials Science Centre, Indian Institute of Technology, Kharagpur 721302
[*]Corresponding author: ncdas@rtc.iitkgp.ernet.in

Characterization

The morphology of the KLBC-dots were examined by high resolution transmission electron microscope HRTEM (JEOL, JEM 2100F, operating voltage 200 kV, Japan). The Fourier transform infrared (FTIR) spectrum of the KLBC-dots were recorded on a FTIR spectrophotometer (Perkin Elmer, model-Spectrum-2, Singapore) in the range of 500-4000 cm^{-1} with resolution of 4 cm^{-1} and 16 scans. Fluorescence studies were measured on a Fluoromax_4C_1052D_4312_FM spectrofluorometer, excitation/emission slits of 2 nm. UV-visible absorption spectrum of the KLBC-dots in aqueous solution was performed using a UV Spectrometer (PerkinElmer, model-2 Singapore, Lambda35). The Auger spectra, elemental composition and mapping of the prepared KLBC-dots were analyzed by ULVAC-PHI, Inc., 370 Enzo, Chigasaki, Kanagawa, Japan. ^{1}H-NMR was performed on Bruker, 600 MHz instrument using tetramethylsilane as an internal standard. Atomic force microscopic image of the KLBC-dots was taken by Agilent 5500 scanning probe microscope after drop casting of KLBC-dots on a silicon wafer substrate. The images were acquired in non-contact tapping mode. Fluorescent microscopic images were taken on Carl Zeiss, Germany using ZEN software.

Optimization of the synthesis conditions

The luminescence property of the C-dots is generally influenced by different factors such as hydrothermal temperature, reaction time, and precursor concentration. Hence, in order to get good optical properties of the KLBC-dots, experimental conditions need to be optimized. Before optimizing KLBC-dots, we have optimized the synthesis of C-dots i.e. C-dots prepared from lemon juice and kappa carrageenan without modification of BKC. As the carbon source, 6 mL lemon juice was taken and the concentration of kappa carrageenan was varied (0.003 M to 0.5 M) after fixing the hydrothermal reaction temperature and time at 180 °C and 7 h respectively. It was observed when the concentration of the kappa carrageenan was 0.02 (M) keeping other two factors/variables (reaction temperature of 180 ^{o}C and time of 7 h) constant, the QY attained a maximum value 54.43 % (Fig. S1a). Noteworthy decrease in QY was noticed when the concentration of the kappa carrageenan was increased above or decreased below 0.02 (M). Thus, 0.02 M concentration has been assumed as critical concentration throughout the whole study. The hydrothermal reaction temperatures investigated in this study were 120, 140, 160, 180, 200, 220 and 240 °C keeping the concentration of kappa carrageenan 0.02 (M) and volume of lemon juice 6 mL, and reaction duration 7 h. As it seen from Fig. S1b, that reaction temperature had intimate relation with the QY of the C-dots with maximum QY of the C-dots (54.43 %) when the reaction temperature was 180 °C. Afterward the effect of reaction time was studied keeping the concentration of kappa carrageenan 0.02 (M) and volume of lemon juice 6 mL, and reaction temperature 180 °C. Fig. S1c clearly unveiled that 7 h of reaction yields the best performance for the C-dots in terms of their QY (54.43 %). Therefore the control experimental conditions for the synthesis of the C-dots are: concentration of kappa carrageenan 0.02 (M), 6 mL lemon juice, reaction temperature 180 °C, and hydrothermal reaction time of 7 h. Now to obtain BKC modified C-dots i.e. KLBC-dots, the concentration of the BKC was altered keeping the concentration of the C-dots 0.87 mg/mL and stirring reaction time 24 h. Fig.S2a showed that change in QY with the change in BKC concentration. Maximum QY 67.54 % was obtained when the concentration of BKC was 0.02 (M) and hence fixed as the optimum conditions. Following this, the stirring reaction time was modulated to understand the effect of reaction time on the QY of the KLBC-dots. For this the stirring reaction time was monitored as 6, 12, 18, 24, 30, 36, and 42 h. The result showed (Fig. S2b) that at 24 h stirring KLBC-dots attained maximum QY (62.54 %) and further increase in stirring time there was no severe change in QY.

Therefore, to acquire KLBC-dots with good luminescent properties the conditions were BKC concentration 0.02 M, C-dots 0.87 mg/mL and stirring reaction time 24 h. Under these conditions, robust KLBC-dots with superior QY (62.54 %) were achieved.

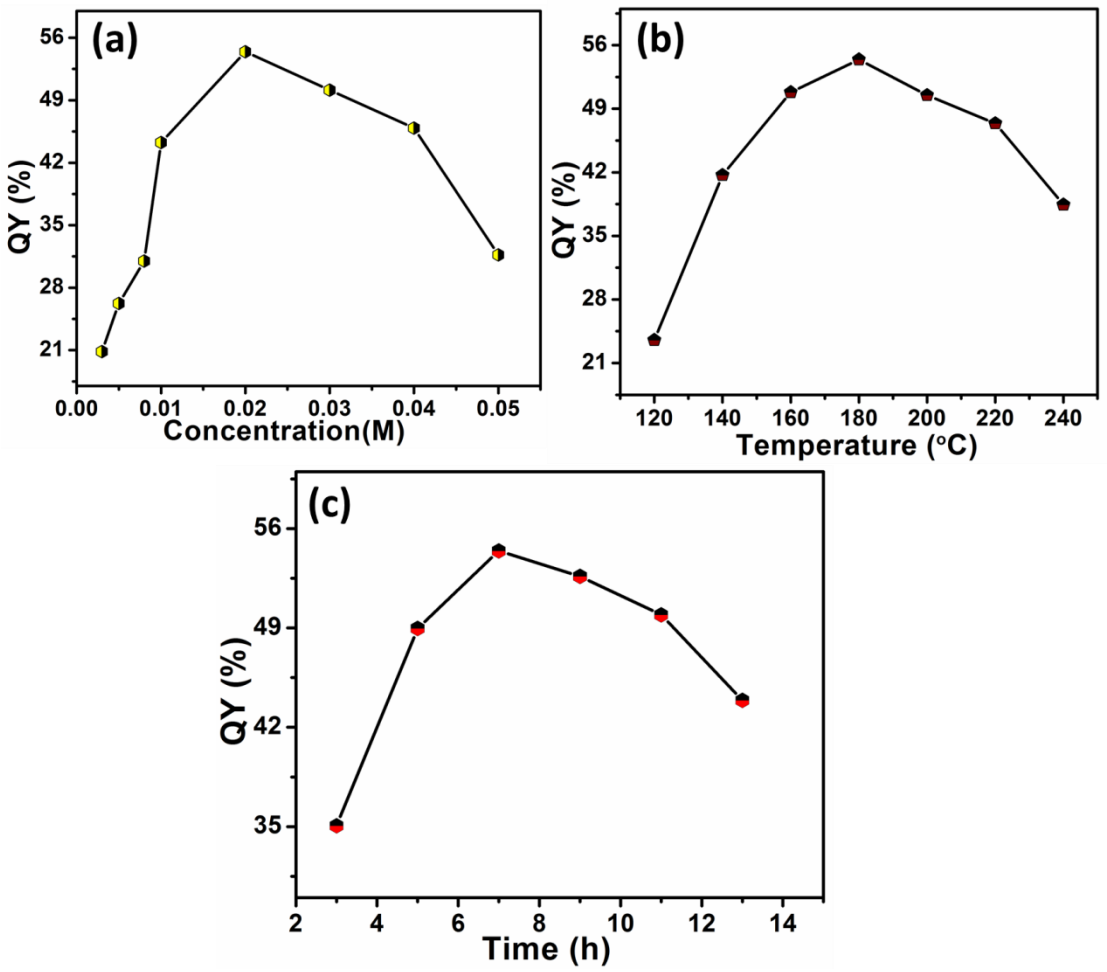

Fig. S1 Quantum yield results by (a) concentration variation of kappa carrageenan (b) temperature of the hydrothermal reaction (from 120 to 240 °C); (c) hydrothermal reaction time (from 1 to 11 h).

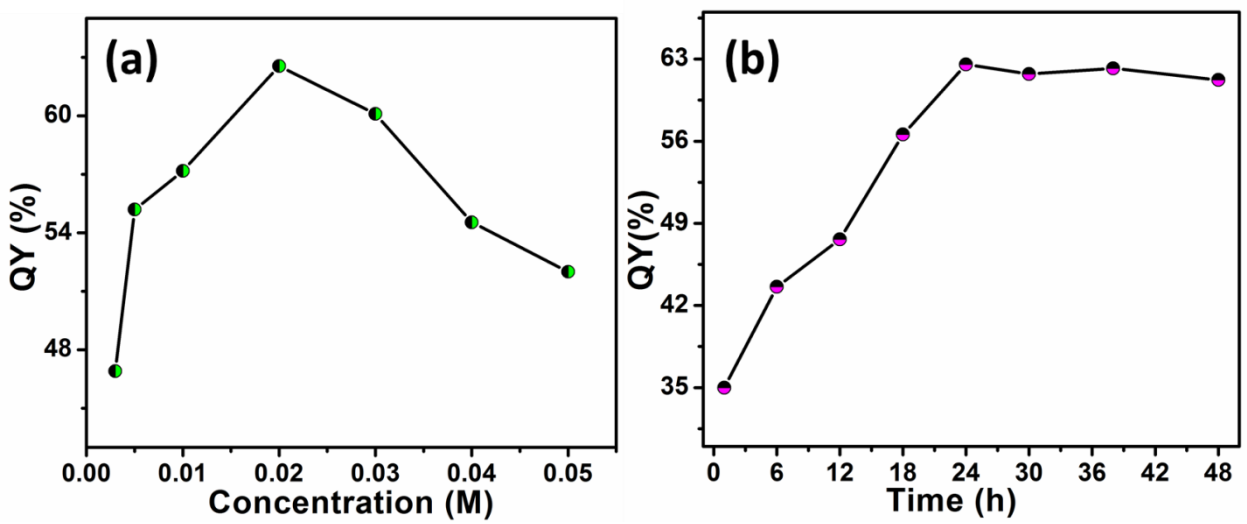

Fig. S2 Quantum yield results by (a) concentration variation BKC (b) Stiring reaction time (from 1 to 48 h).

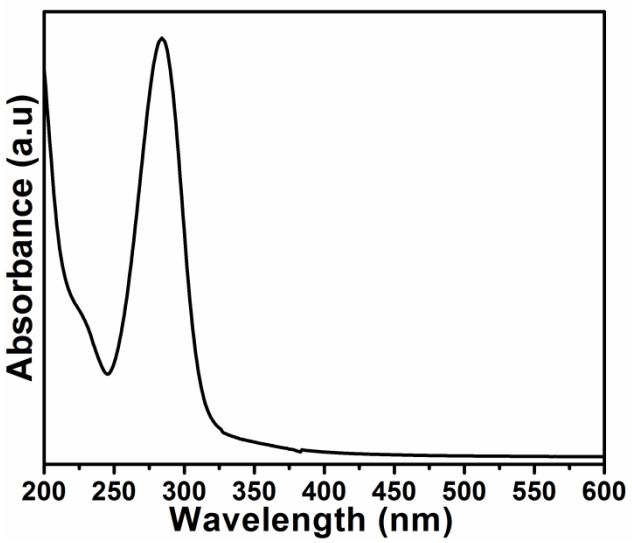

Fig. S3 UV-Vis absorption spectrum of the C-dots.

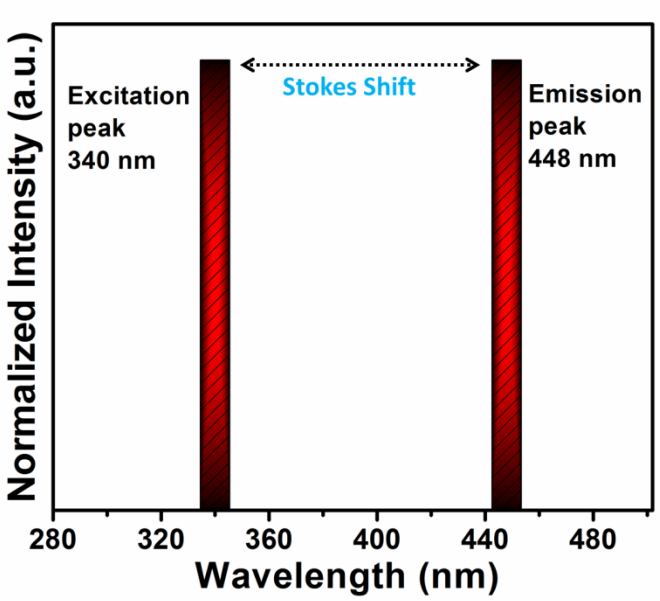

Fig. S4 Excitation and emission peak and Stokes Shift of the KLBC-dots.

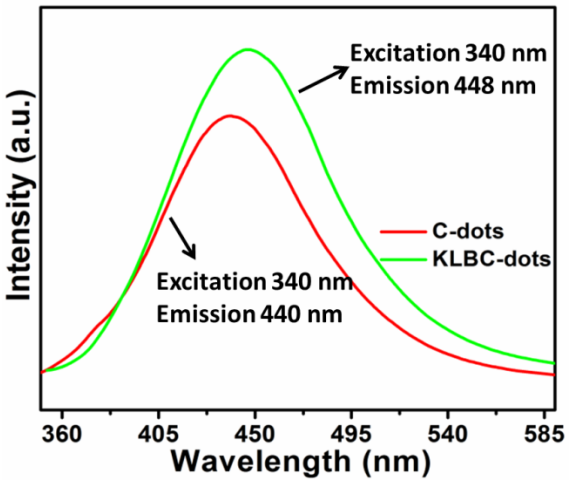

Fig. S5 Fluorescence emission spectra of C-dots and KLBC-dots.

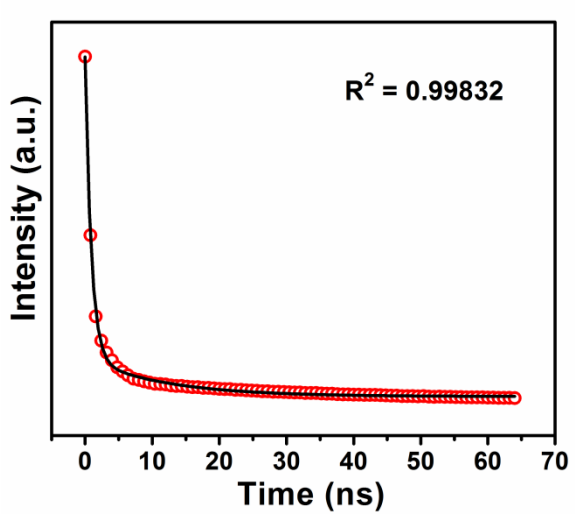

Figure S6 FL decay profile for KLBC-dots at 295 nm excitation.

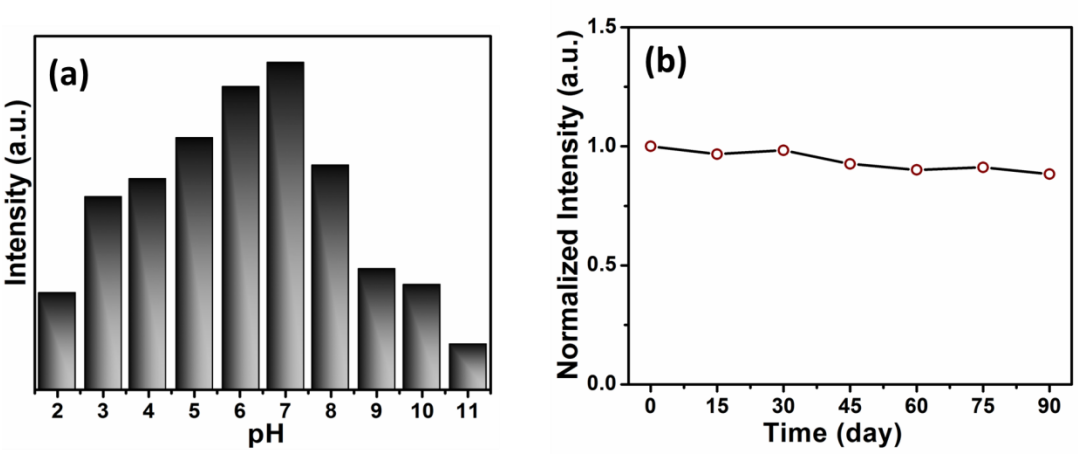

Fig. S7 (a) Effect on FL intensity of the KLBC-dots at different pH values. (b) Effect of time in the fluorescence property of the KLBC-dots. All emissions were collected at 448 nm, excitation 340 nm.

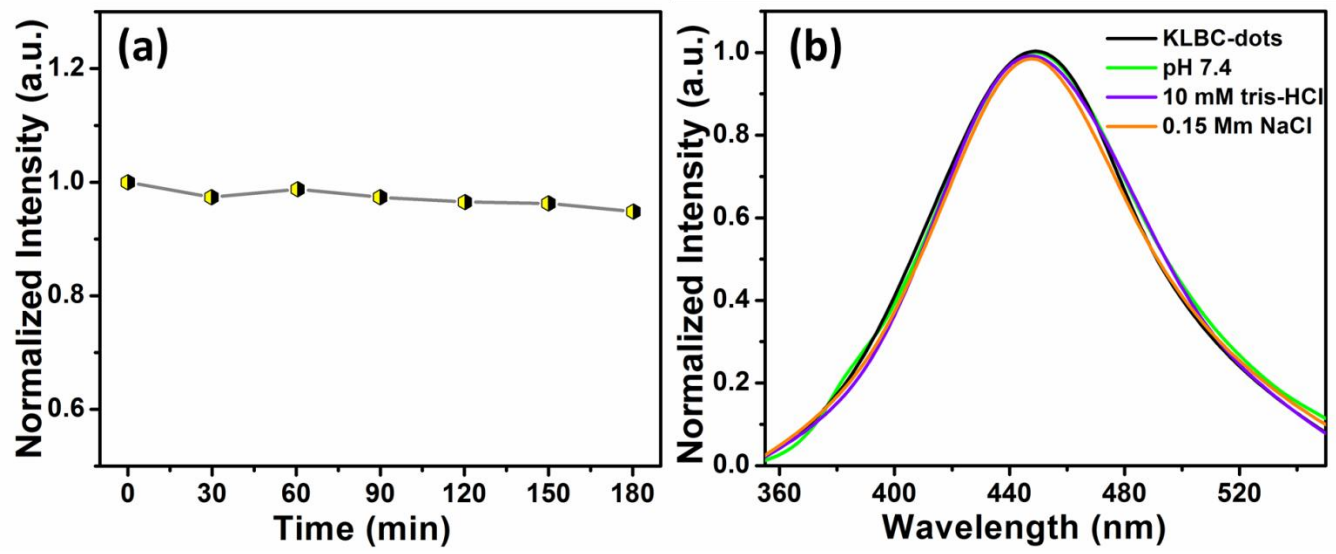

Fig. S8 (a) Stability of the KLBC-dots under UV light exposure, and (b) Effect of FL intensity of the KLBC-dots under various physiological conditions. All emission spectra were collected at 448 nm, excitation 340 nm.

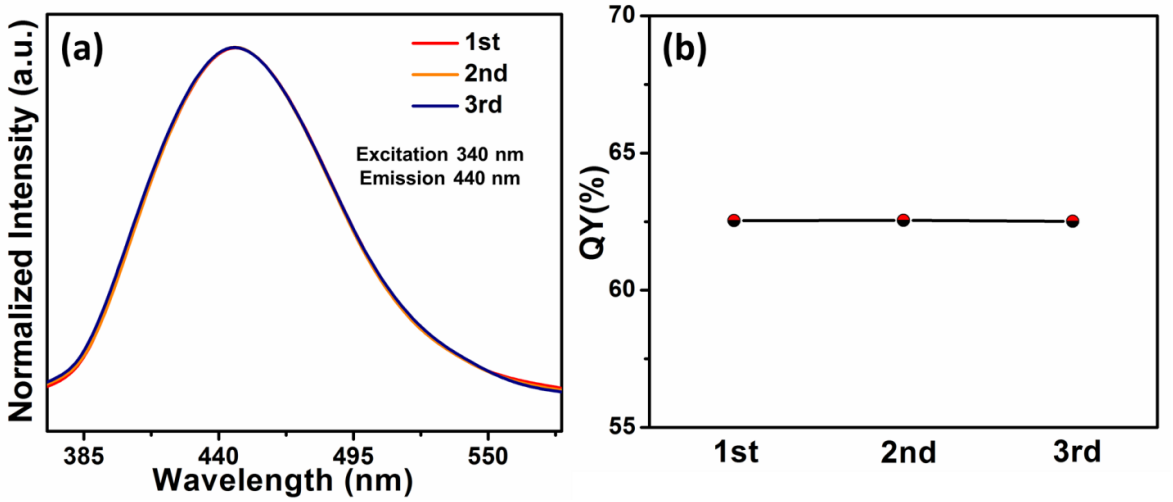

Fig. S9 (a) Emission spectra and (b) quantum yield of the KLBC-dots synthesis in triplicate.

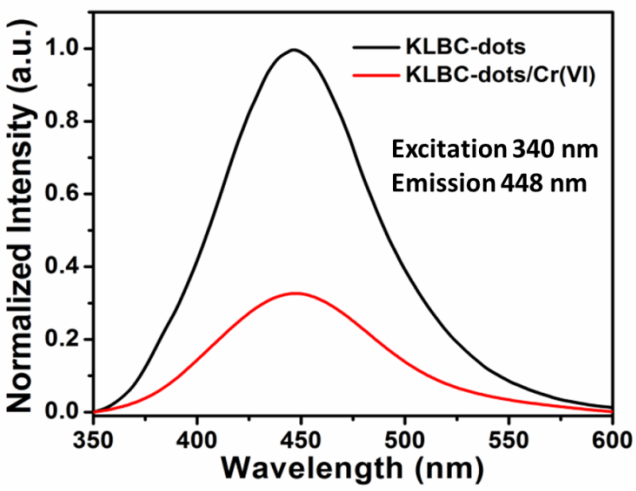

Fig. S10 Fluorescence emission spectra of KLBC-dots in absence and presence of Cr (VI).

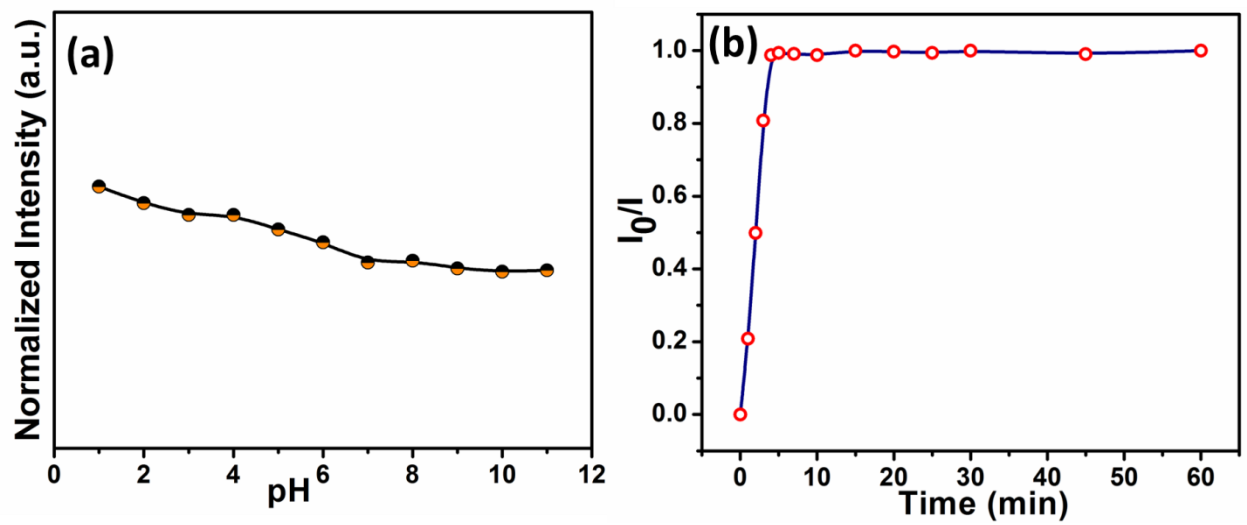

Fig. S11 (a) pH effect on quenching of KLBC-dots by Cr(VI). (b) Incubation time of KLBC-dots with Cr(VI).

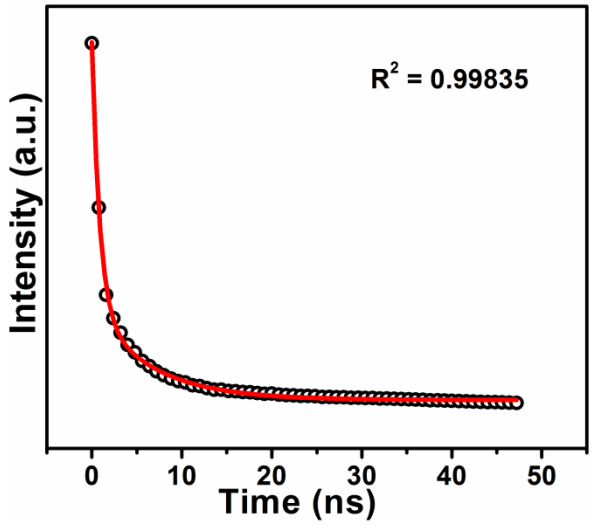

Fig. S12 FL decay profile for KLBC-dots in presence of 50µM Cr(VI).

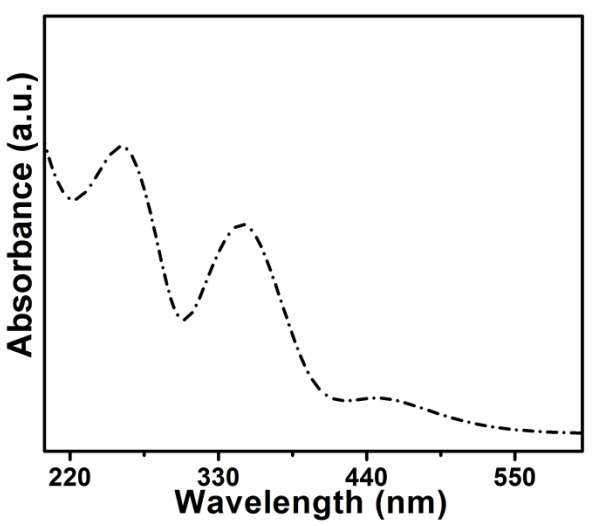

Fig. S13 UV-Vis absorption spectrum of the Cr(VI).

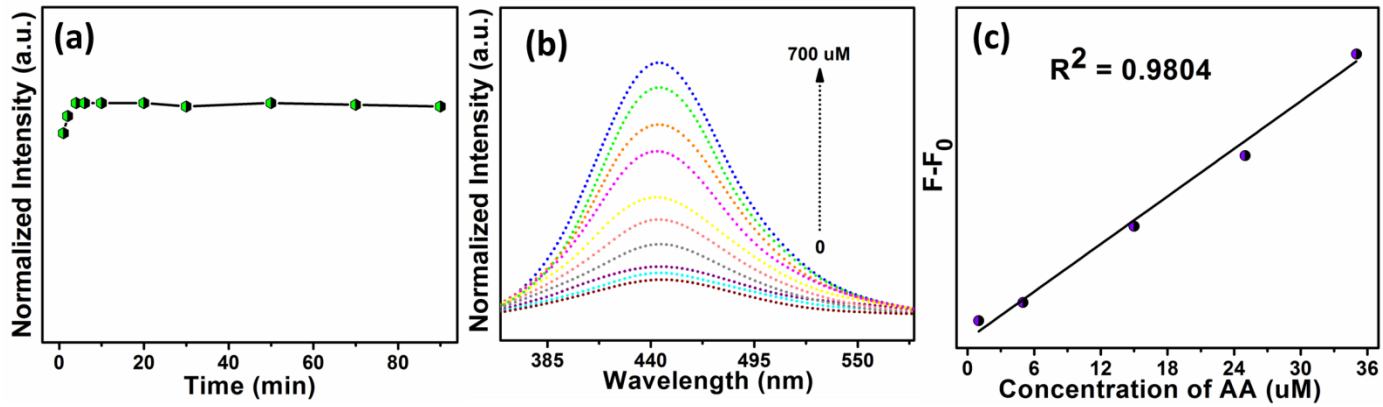

Fig. S14 (a) Incubation time of KLBC-dots/Cr with AA. (b) Fluorescence spectra of KLBC-dots− Cr(VI) system in different concentrations of AA (from bottom to top): 0, 1, 5, 15, 25, 35, 100, 200, 500, and 700 μM. (c) Relationship between *F*- F_0 and concentration of AA concentration in the 1 to 35 μM range. All emission spectra at 448 nm were collected at 340 nm excitation. KLBC-dots: 0.42 mg mL^{-1}; Cr(VI): 50 μM.

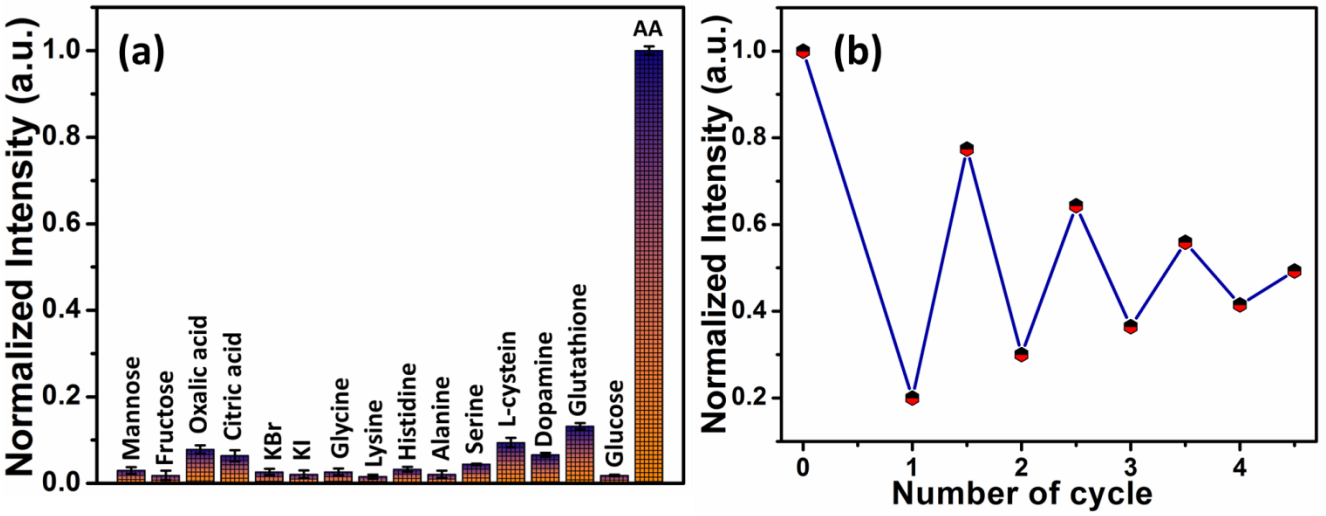

Fig. S15 (a) Selectivity of sensing system towards AA and other potential interference species in the KLBC-dots/Cr(VI) system (Cr(VI) concentration, 120 μM; KLBC-dots concentration, 0.38 mg/mL, species concentration, 120 μM). (b) Changes in the fluorescence intensity of KLBC-dots cycled by adding Cr(VI) and AA. Excitation 340 nm and emission 448 nm; Error bars represent the standard deviation of five independent experiments (n = 5).

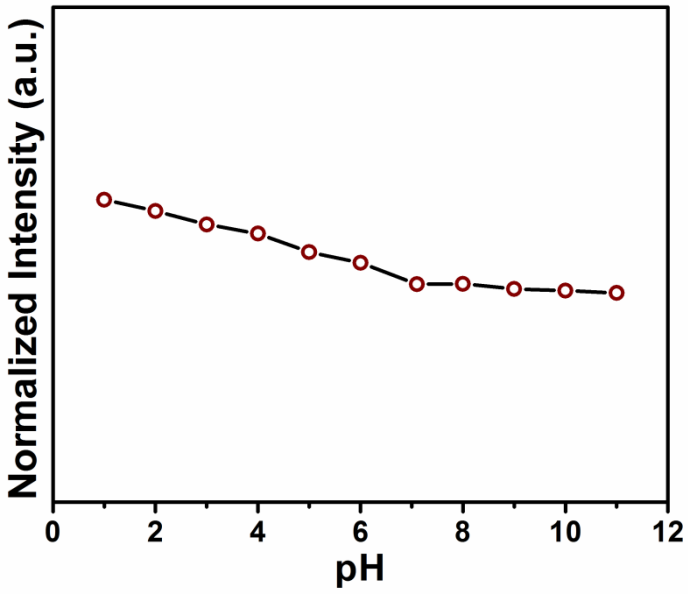

Fig. S16 Influence of pH on quenching of KLBC-dots by Cr(VI) in river water.

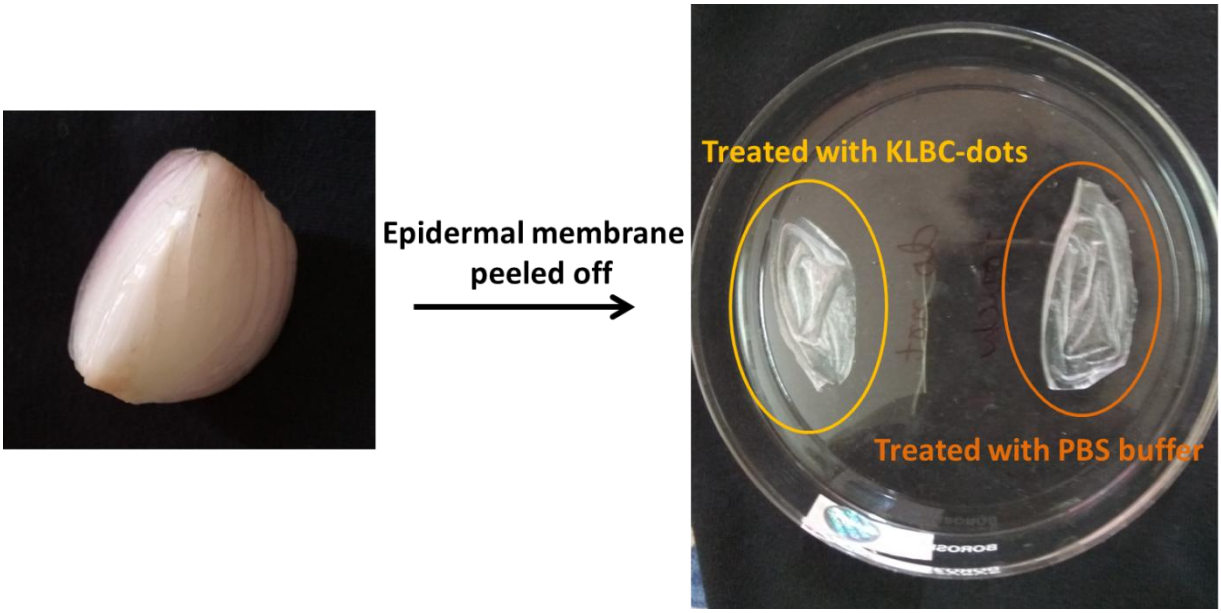

Fig. S17 Onion epidermal membrane treated with KLBC-dots (marked with yellow), and PBS buffer (marked with orange).

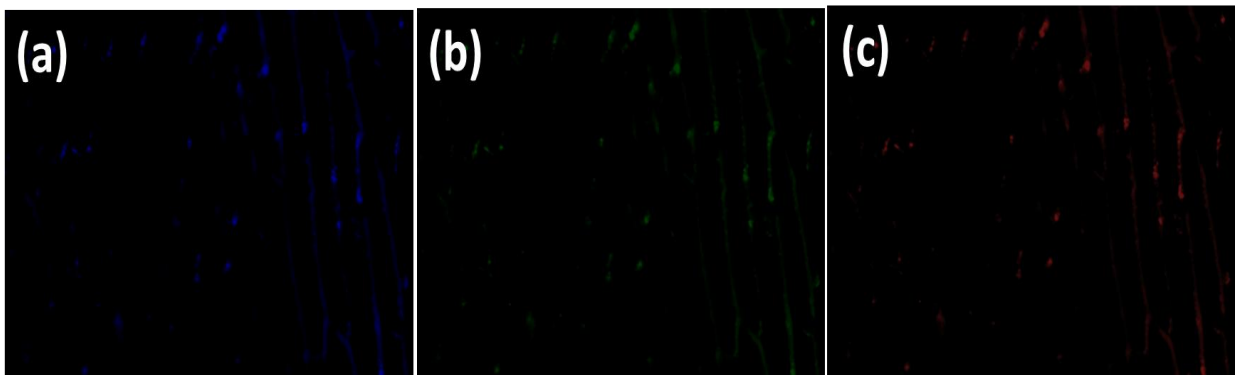

Fig. S18 Fluorescence microscopy images of onion epidermal cells treated with KLBC-dots + 25 μM Cr(VI) under excitation filters (a) 330–380 nm (c) 450–490 nm (d) 510–560 nm using ZEN software.

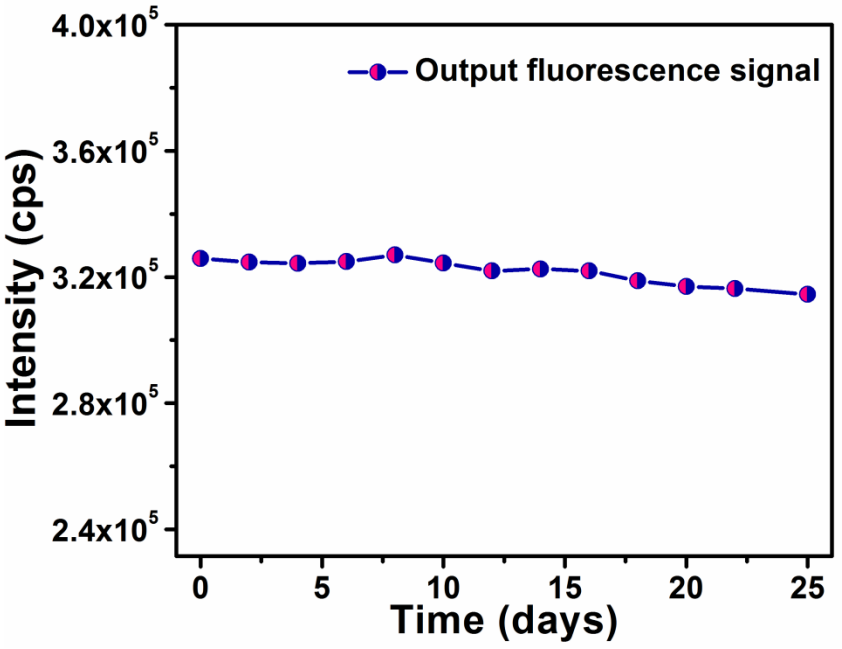

Fig. S19 Stability of the output signal

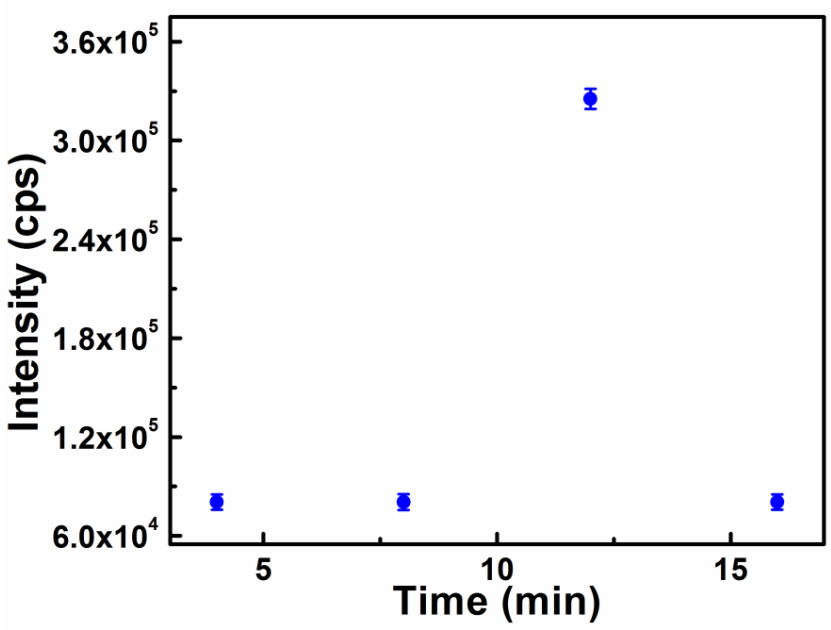

Fig. S20 The error bar represents standard deviation of three replicates.

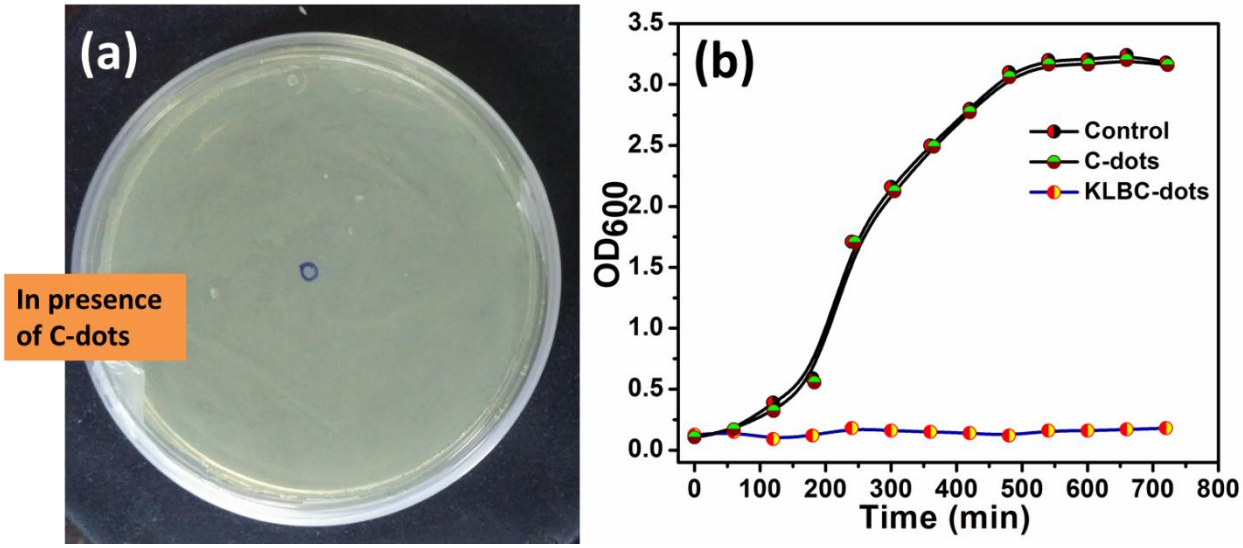

Fig. S21 (a) Image of antibacterial activity of C-dots by the disc diffusion method. (b) Bacterial growth curve of control, in presence of C-dots, and KLBC-dots.

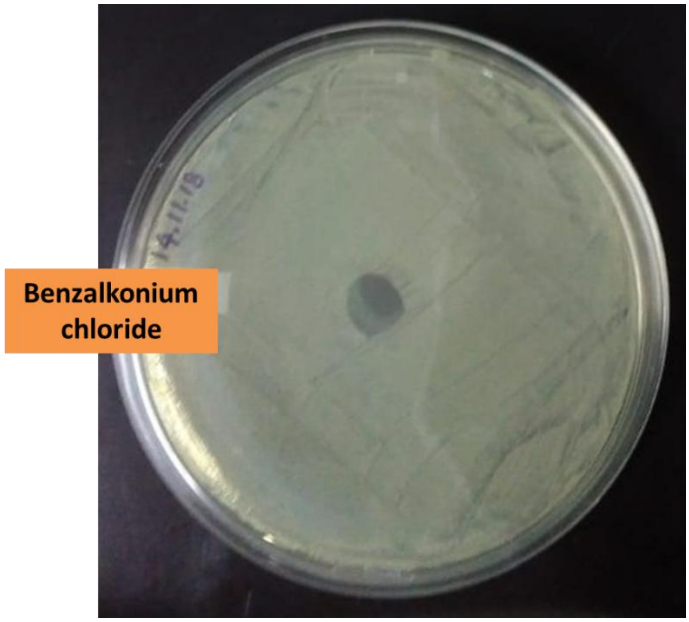

Fig. S22 Digital photograph of agar plate with inhibition zone of benzalkonium chloride against *E. coli*.

Table S1 Comparison of synthesis methods and nitrogen content of different C-dots

Synthetic method	**Precursor**	**Nitrogen content (%)**	**Reference**
Hydrothermal (180^{o}C)	Polythiophene and diphenyl diselenide	0.58	[1]
Acid vapour cutting strategy	2-methylimidazole and Zn $(NO_3)_2 \cdot 6H_2O$, SiO_2 griddle, concentrated HNO_3	4.9 %	[2]

In an ammonia atmosphere (530^oC)	TiO_2 nanoparticle, fluorine-doped tin oxide, ammonia, ammonia solution	1.94 %	[3]
Hydrothermal ($200\ ^oC$)	Lemon juice and L-arginine	4.96 %	[4]
Sol-gel method produce TiO_2/N nanoparticle, sensitized with CdSe quantum dots	Hexamethylenetetramine, thioglycolic acid	0.6 %	[5]
Hydrothermal and ion exchange process followed by calcination at 450 °C under Ar atmosphere.	$Na_2Ti_3O_7$ nanorods/ C-dots (prepared by the electrochemical anodic oxidation of alcohol) composite	1.7 %	[6]

Table S2 The fluorescence lifetimes of the KLBC-dots

Sample	**Excitation (nm)**	**τ_1 (ns)**	**τ_2 (ns)**	**A_1 (%)**	**A_2 (%)**	**τ_{avg} (ns)**
KLBC-dots	295	0.91	11.14	87.45	12.82	7.47
	375	6.43	0.75	48.19	51.81	5.79

Table S3 Comparison of various types of C-dots synthesis from different precursors

Precursors	Synthesis method	Size (nm)	PL color	Emission nature	Reference
Glucose	Hydrothermal (200^{o}C)	3.83	Green	Excitation dependent	[7]
CCl_4, Quinol, NaOH, Ethanol	Solvothermal (200^{o}C	3-5	Blue	-	[8]
Grape juice	Hydrothermal (180^{o}C)	2.7	Green	Excitation dependent	[9]
Citric acid, Urea	Hydrothermal (160^{o}C)	5	Blue	Excitation independent	[10]
Willow bark	Hydrothermal (200^{o}C)	1-4	Blue	Excitation dependent	[11]
Citric acid, tris(hydroxymethyl)aminomethane, zinc acetate	Hydrothermal (200^{o}C)	1.5–5 nm	Bluish white	Excitation independent	[12]
Acrylic acid, 1,2-ethanediamine	Microwave (700W)	2.0-3.2	Blue	Excitation dependent	[13]
Kappa Carrageenan, Lemon juice, BKC	Hydrothermal	4.5	Green	Both excitation dependent and independent	This work

Table S4 Double-exponential fitting of KLBC-dots and KLBC-dots/Cr(VI) decay curves.

Sample name	KLBC-dots	KLBC-dots/Cr(VI)
τ_1 (ns) / A_1 (%)	6.43/48.19	6.60/31.62
τ_2 (ns) / A_2 (%)	0.75/51.81	0.87/68.38
τ (ns)	5.79	5.33

Table S5 Detection of AA in Vitamins C tablet

Sample	Spiked (μM)	Found (μM)	Recovery (%)	RSD (%)
KLBC-dots	50.00	48.16	96	0.93
	100.00	102.52	102	1.04
	150.00	151.54	101	1.07
	250.00	247.73	99	0.95

Reference

[1] M. Lan, S. Zhao, Z. Zhang, L. Yan, L. Guo, G. Niu, J. Zhang, J. Zhao, H. Zhang, P. Wang, Two-photon-excited near-infrared emissive carbon dots as multifunctional agents for fluorescence imaging and photothermal therapy, Nano Research 10 (2017) 3113-3123.

[2] H. Xu, S. Zhou, L. Xiao, H. Wang, S. Li, Q. Yuan, Fabrication of a nitrogen-doped graphene quantum dot from MOF-derived porous carbon and its application for highly selective fluorescence detection of Fe 3+, Journal of Materials Chemistry C 3 (2015) 291-297.

[3] J. Hensel, G. Wang, Y. Li, J.Z. Zhang, Synergistic effect of CdSe quantum dot sensitization and nitrogen doping of TiO2 nanostructures for photoelectrochemical solar hydrogen generation, Nano Letters 10 (2010) 478-483.

[4] P. Das, S. Ganguly, M. Bose, S. Mondal, A.K. Das, S. Banerjee, N.C. Das, A simplistic approach to green future with eco-friendly luminescent carbon dots and their application to fluorescent nano-sensor 'turn-off'probe for selective sensing of copper ions, Materials Science and Engineering: C 75 (2017) 1456-1464.

[5] T. Lopez-Luke, A. Wolcott, L.-p. Xu, S. Chen, Z. Wen, J. Li, E. De La Rosa, J.Z. Zhang, Nitrogen-doped and CdSe quantum-dot-sensitized nanocrystalline TiO2 films for solar energy conversion applications, The Journal of Physical Chemistry C 112 (2008) 1282-1292.

[6] Y. Yang, X. Ji, M. Jing, H. Hou, Y. Zhu, L. Fang, X. Yang, Q. Chen, C.E. Banks, Carbon dots supported upon N-doped TiO 2 nanorods applied into sodium and lithium ion batteries, Journal of Materials Chemistry A 3 (2015) 5648-5655.

[7] Z.-C. Yang, M. Wang, A.M. Yong, S.Y. Wong, X.-H. Zhang, H. Tan, A.Y. Chang, X. Li, J. Wang, Intrinsically fluorescent carbon dots with tunable emission derived from hydrothermal treatment of glucose in the presence of monopotassium phosphate, Chemical Communications 47 (2011) 11615-11617.

[8] J. Zhou, P. Lin, J. Ma, X. Shan, H. Feng, C. Chen, J. Chen, Z. Qian, Facile synthesis of halogenated carbon quantum dots as an important intermediate for surface modification, RSC Advances 3 (2013) 9625-9628.

[9] H. Huang, Y. Xu, C.-J. Tang, J.-R. Chen, A.-J. Wang, J.-J. Feng, Facile and green synthesis of photoluminescent carbon nanoparticles for cellular imaging, New Journal of Chemistry 38 (2014) 784-789.

[10] X. Li, S. Zhang, S.A. Kulinich, Y. Liu, H. Zeng, Engineering surface states of carbon dots to achieve controllable luminescence for solid-luminescent composites and sensitive Be 2+ detection, Scientific Reports 4 (2014) 4976.

[11] X. Qin, W. Lu, A.M. Asiri, A.O. Al-Youbi, X. Sun, Green, low-cost synthesis of photoluminescent carbon dots by hydrothermal treatment of willow bark and their application as an effective photocatalyst for fabricating Au nanoparticles–reduced graphene oxide nanocomposites for glucose detection, Catalysis Science & Technology 3 (2013) 1027-1035.
[12] P. Das, S. Ganguly, M. Bose, S. Mondal, S. Choudhary, S. Gangopadhyay, A.K. Das, S. Banerjee, N.C. Das, Zinc and nitrogen ornamented bluish white luminescent carbon dots for engrossing bacteriostatic activity and Fenton based bio-sensor, Materials Science and Engineering: C 88 (2018) 115-129.
[13] P. Zhang, W. Li, X. Zhai, C. Liu, L. Dai, W. Liu, A facile and versatile approach to biocompatible “fluorescent polymers” from polymerizable carbon nanodots, Chemical Communications 48 (2012) 10431-10433.